

General Relativistic Modeling of Magnetized Jets from Accreting Black Holes

Alexander Tchekhovskoy¹, Jonathan C. McKinney² and Ramesh Narayan³

¹Center for Theoretical Science, Jadwin Hall, Princeton University, Princeton, NJ 08544, USA; Princeton Center for Theoretical Science Fellow

²Kavli Institute for Particle Astrophysics and Cosmology, Stanford University, P.O. Box 20450, MS 29, Stanford, CA 94309, USA

³Institute for Theory and Computation, Harvard-Smithsonian Center for Astrophysics, 60 Garden Street, MS 51, Cambridge, MA 02138, USA

E-mail: atchekho@princeton.edu

Abstract. Recent advances in general relativistic magnetohydrodynamic modeling of jets offer unprecedented insights into the inner workings of accreting black holes that power the jets in active galactic nuclei (AGN) and other accretion systems. I will present the results of recent studies that determine spin-dependence of jet power and discuss the implications for the AGN radio loud/quiet dichotomy and recent observations of high jet power in a number of AGN.

1. Introduction

Relativistic jets are one of the most spectacular manifestations of black hole (BH) accretion. Jet-producing accretion systems span 9 decades in central BH mass: from stellar-mass BHs in black hole binaries (BHs) and gamma-ray bursts (GRBs) to supermassive BHs in active galactic nuclei (AGN). If a single physical mechanism is responsible for producing jets throughout the BH mass spectrum, it must be robust and scale invariant. Magnetic fields are a promising agent for jet production because they are abundant in astrophysical plasmas and because the properties of magnetically-powered jets scale trivially with BH mass [1–5].

How are jets magnetically launched? Figure 1 shows a cartoon depiction of this. Consider a vertical magnetic field line attached on one end to a perfectly conducting sphere, which represents the central compact object, and on the other end to a perfectly conducting “ceiling” which represents the ambient medium (panel a). As the sphere is spinning, after N turns the initially vertical field line develops N toroidal field loops (panel b). This magnetic spring pushes against the ceiling due to the pressure of the toroidal field. As more toroidal loops form and the toroidal field becomes stronger, the spring pushes away the ceiling and accelerates any plasma attached to it along the rotation axis, forming a jet (panels (c) and (d) in Figure 1, see the caption for details). In the case when the central body is a black hole, which does not have a surface, the rotation of space-time causes the rotation of the field lines, and jets form in a similar fashion via a process referred to as Blandford-Znajek mechanism (BZ, hereafter) [1].

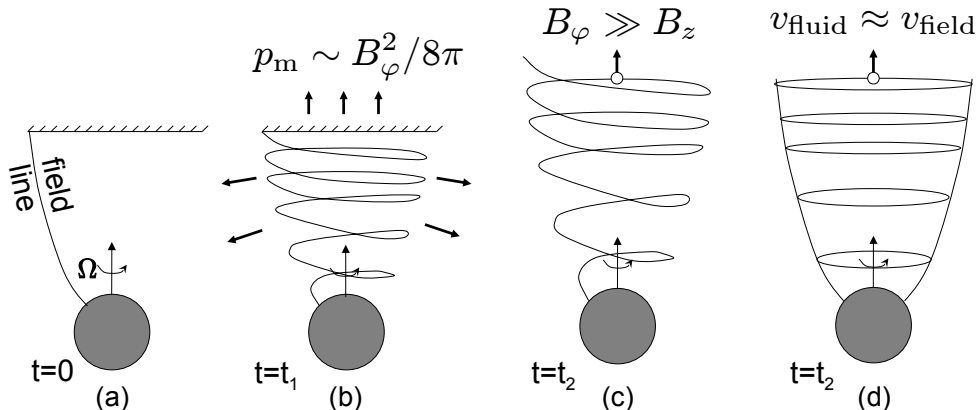


Figure 1. Illustration of jet formation by magnetic fields. (a) Consider a purely poloidal (i.e., $B_\varphi = 0$) field line attached on one end to a stationary “ceiling” (which represents the ambient medium and is shown with hashed horizontal line) and on the other end to a perfectly conducting sphere (which represents the central BH or disk and is shown with grey filled circle) rotating at an angular frequency Ω . (b) After N rotations, at time $t = t_1$, the initially purely poloidal field line develops N toroidal loops. This magnetic spring pushes against the “ceiling” with an effective pressure $p_m \sim B_\varphi^2/8\pi$ due to the toroidal field, B_φ . As time goes on, more toroidal loops form, and the toroidal field becomes stronger. (c) At some later time, $t = t_2$, the pressure becomes so large that the spring pushes away the “ceiling” and accelerates the plasma attached to it along the rotation axis, forming a jet. Asymptotically far from the center, the toroidal field is the dominant field component and determines the dynamics of the jet. (d) It is convenient to think of the jet as a collection of toroidal field loops that slide down the poloidal field lines and accelerate along the jet under the action of their own pressure gradient and hoop stress. The rotation of the sphere continuously twists the poloidal field into new toroidal loops at a rate that, in steady state, balances the rate at which the loops move downstream.

2. Radio-Loud/Quiet Dichotomy of Active Galactic Nuclei

Despite decades of research, we still do not understand what determines jet power in accretion systems or how to accurately infer jet powers observationally [6–11]. There are a number of unresolved puzzles. For the same nuclear B-band luminosity, radio-loud (RL) AGN have a factor of 10^3 higher total (core plus extended) radio luminosity than radio-quiet (RQ) AGN. Figure 3 in [12] clearly shows that these two flavors of AGN follow two well-separated tracks on the radio-loudness diagram, which shows the radio-loudness parameter, \mathcal{R} , the ratio of radio to optical luminosities at specified frequencies vs. the Eddington ratio, λ . This dichotomy is especially pronounced at low $\lambda \lesssim 0.01$ when the accretion systems are thought to be in a radiatively inefficient state of accretion, with a geometrically thick accretion disk. For higher λ -values, accretion systems can undergo spectral state transitions (as seen in BHBs, [13]), which might cause differences in \mathcal{R} . Therefore, we limit ourselves to low- λ systems.

If total (core plus extended) radio luminosity is a tracer of jet power, could the dichotomy be due to the differences in the spin of central BHs that power the relativistic jets in RL and RQ AGN [14]? Characteristic values of BH spin in RQ AGN, which lie predominantly at the centers of spiral galaxies, can be quite low, $|a| \lesssim 0.3$. This can be understood if the orientation of angular momentum accreted by the central BHs changes randomly between accretion events [15]. On the other hand, the spin of central BHs in RL AGN, which are hosted predominantly by elliptical galaxies, can be much higher, $a \sim 1$ [15]. Can this difference in BH spin lead to a factor of 10^3 dichotomy?

In the presence of large-scale magnetic fields, rotating BHs produce outflows via the BZ

mechanism, which extracts BH rotational energy at a rate,

$$P_{\text{BZ}} = \frac{\kappa}{4\pi c} \Phi_{\text{BH}}^2 \frac{a^2}{16r_g^2} \quad (\text{standard BZ formula, low-spin limit, } a^2 \ll 1), \quad (1)$$

where $\kappa \approx 0.05$ weakly depends on magnetic field geometry, Φ_{BH} is the magnetic flux through the BH horizon, and $r_g = GM/c^2$ is BH gravitational radius [1]. This low-spin approximation, which we refer to as the standard BZ formula, remains accurate up to $a \lesssim 0.5$ [16, 17], which can be seen in Figure 2. Clearly, the $\propto a^2$ scaling does not appear steep enough to explain the 10^3 dichotomy: BH power varies by a factor of ~ 10 if a varies from 0.3 to 1. Can the power dependence becomes steeper as $a \rightarrow 1$? Figure 2 illustrates that an expansion in the powers of BH angular frequency, $\Omega_{\text{H}} = ac/2r_{\text{H}}$,

$$P_{\text{BZ}} = \frac{\kappa}{4\pi c} \Phi_{\text{BH}}^2 \Omega_{\text{H}}^2 f(\Omega_{\text{H}}) \quad (\text{BZ6 formula, accurate for all values of } a), \quad (2)$$

remains accurate up to $a \lesssim 0.95$ for $f = 1$ (referred to as the BZ2 formula), where $r_{\text{H}} = r_g[1 + (1 - a^2)^{1/2}]$ is BH horizon radius. Equation (2) with $f(\Omega_{\text{H}}) \approx 1 + 1.38(\Omega_{\text{H}}r_g/c)^2 - 9.2(\Omega_{\text{H}}r_g/c)^4$ remains accurate for all spins [18], and this gives us our BZ6 formula. Figure 2 shows that while at small spin the BZ6 formula (2) and the standard BZ formula (1) agree, as $a \rightarrow 1$ the BZ6 formula gives about 3 times more power. However, the spin dependence is still not steep enough to explain the dichotomy: BH power varies by a factor of ~ 30 if a varies from 0.3 to 1.

So far we considered razor-thin accretion disks, which is an implicit assumption behind the above expressions for power, eqs. (1)–(2). However, disks in low-luminosity AGN are thick, with disk angular thickness as large as $H/R \sim 1$ (including disk body and magnetized corona). Such a thick disk mass-loads equatorial field lines on the BH, so that they become part of a sub-relativistic disk wind, and only the magnetic flux in the highly magnetized funnel above and below the disk contributes to the jet. If the total magnetic flux, Φ_{BH} , through the BH is held constant, this disk occultation effect can cause a much steeper spin-dependence of jet power, $P_{\text{jet}} \propto \Omega_{\text{H}}^4$, as is seen in Fig. 2. Then, variation of power by a factor of 10^3 is possible, which can explain the radio loud/quiet dichotomy of AGN [18].

3. What Sets Jet Power in Black Hole Accretion Systems?

We have shown that BH power is directly proportional to the square of BH magnetic flux, Φ_{BH} , and the square of BH angular frequency, Ω_{H} (see eq. 2), with small corrections beyond $a \gtrsim 0.95$. In Nature, Φ_{BH} is a free parameter, whose value is poorly observationally constrained. Clearly, we have $\Phi_{\text{BH}}^2 \propto \dot{M}c^2$. But what sets the dimensionless ratio, $\phi_{\text{BH}}^2 = \Phi_{\text{BH}}^2/\dot{M}r_g^2c$, which characterizes the degree of inner disk magnetization and controls energy extraction from the BH [19–24]? Using ϕ_{BH} , we define BZ efficiency as BZ6 power (eq. 2) normalized by $\dot{M}c^2$:

$$\eta_{\text{BZ}} = \frac{\langle P_{\text{BZ}} \rangle}{\langle \dot{M} \rangle c^2} \times 100\% = \frac{\kappa}{4\pi} \langle \phi_{\text{BH}}^2 \rangle \left(\frac{\Omega_{\text{H}}r_g}{c} \right)^2 f(\Omega_{\text{H}}) \times 100\%, \quad (3)$$

where $\langle \dots \rangle$ is a time-average. Previous GRMHD simulations found $\eta_{\text{BZ}} \lesssim 20\%$, even for nearly maximally spinning BHs [25–28]. Are larger values of η_{BZ} possible? This is an especially important question since observations suggest that some AGN produce jets and winds at a high efficiency, $\eta = (P_{\text{jet}} + P_{\text{wind}})/\langle \dot{M}c^2 \rangle \times 100\% \gtrsim 100\%$ [6–10], where P_{jet} and P_{wind} are jet and wind powers, respectively. Are BHs capable of powering such highly efficient outflows? We tested this with global time-dependent GRMHD accretion disk-jet simulations for different values of BH spin. As is standard, we initialized the simulations with an equilibrium hydrodynamic torus around a spinning BH and inserted a weak, purely poloidal ($B_{\varphi} = 0$) magnetic field loop into the

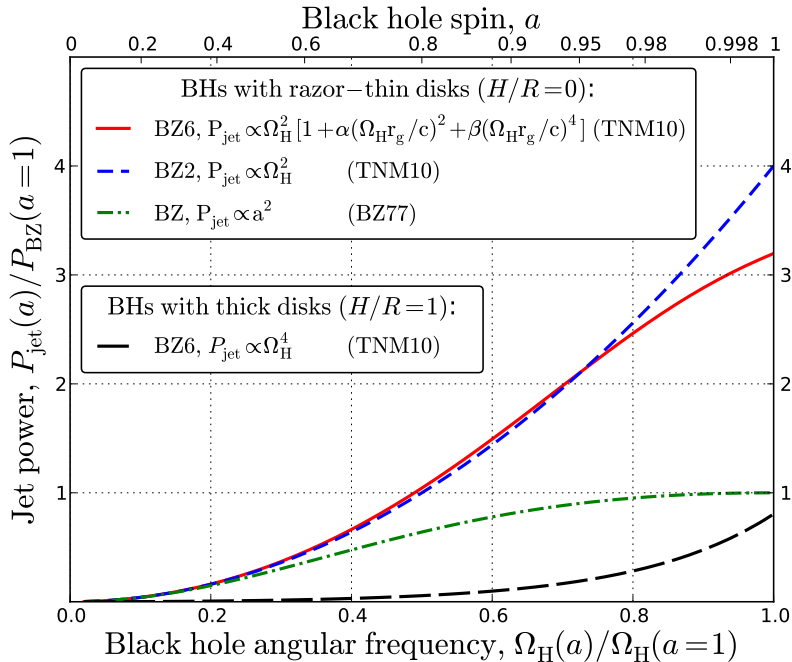


Figure 2. Comparison of various approximations for jet power, P_{jet} , versus BH angular frequency, Ω_{H} (lower x -axis), and BH spin, a (upper x -axis). All powers are normalized to the maximum achievable power in the standard low-spin BZ approximation, $P_{\text{jet}} \propto a^2$, which is shown with dot-dashed green line. The standard BZ approximation remains accurate only for moderate values of spin, $a \lesssim 0.5$, and for maximally-spinning BHs ($a = 1$) it under-predicts the true jet power by a factor of ≈ 3 . This can be seen by comparing to the BZ6 approximation, $P_{\text{jet}} \propto \Omega_{\text{H}}^2 [1 + \alpha(\Omega_{\text{H}} r_g/c)^2 + \beta(\Omega_{\text{H}} r_g/c)^4]$, which is shown with red solid line and which is uniformly accurate for all values of a (the constant factors, $\alpha \approx 1.38$ and $\beta \approx -9.2$, are obtained in [18]). BZ2 approximation, $P_{\text{jet}} \propto \Omega_{\text{H}}^2$, shown with blue short dashed line, is accurate up to $a \lesssim 0.95$, beyond which it requires a modest correction. If a BH is surrounded by a thick accretion disk, the disk intercepts BH power that is emitted into a meridional band occulted by the disk. This reduces jet footprint and power relative to the full BH power for razor-thin disks given above and shown with red solid line (see also [18]), provided that BH magnetic flux is held constant. The resulting BZ6 power for thick disks, with characteristic angular thickness $H/R = 1$ expected in low luminosity AGN, is shown with long dashed black curve. Disk occultation effect on jet power is most pronounced at low spins: it causes a substantial steepening of jet power dependence on spin and can explain a factor of 10^3 radio loud/quiet dichotomy of AGN.

torus. Clearly, jet efficiency (eq. 3) depends on the magnetic flux, and time-dependent numerical simulations show that the larger the large-scale vertical magnetic flux in the initial torus, the more efficient the jets [25, 29–31]. To maximize jet efficiency, we populated the torus with a much larger magnetic flux than in previous work. In fact, our torus contained more magnetic flux than the inner disk can push into the BH. The outcome for BH spin $a = 0.99$ is shown in Figure 3. The magnetorotational instability (MRI, [32]) brings gas and magnetic flux to the BH, and an accretion disk of angular density scale height, $h/r \approx 0.3$, forms. Figure 3(d),(e) shows that both ϕ_{BH} and η increase until $t \approx 6000 r_g/c$, beyond which they saturate and oscillate around the mean, with time-average $\eta \approx 140\%$. At this time, the BH is saturated with magnetic flux, and the magnetic field on the hole is so strong that it obstructs the accretion and leads to a magnetically-arrested disk, MAD [19, 23, 24, 33–37]. In this state both BH dimensionless magnetic flux, ϕ_{BH} , and outflow efficiency, η , are maximum, so it is not surprising that we find

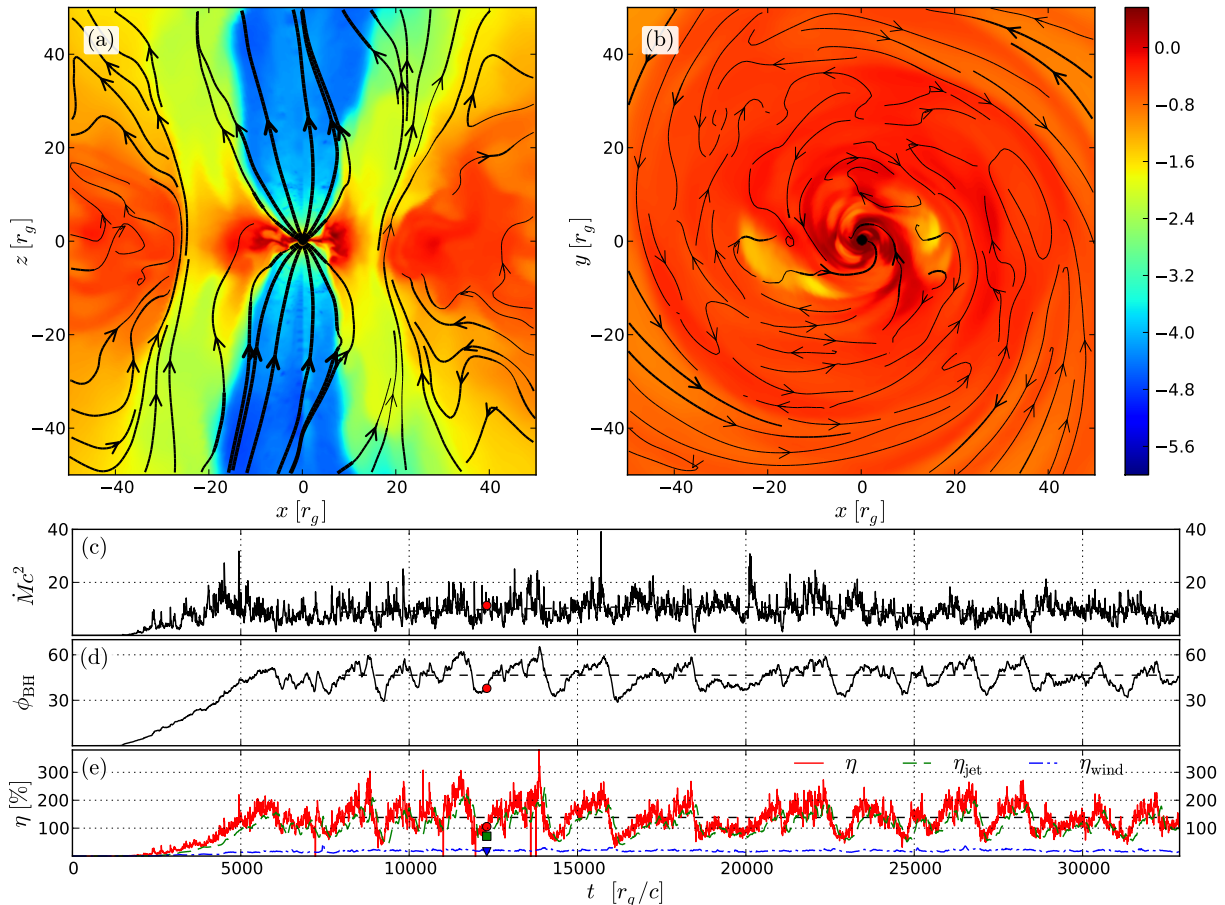


Figure 3. A snapshot and time-dependence of a magnetically-arrested accretion disk [19]. A movie is available at <http://youtu.be/nRGCNaWST5Q>. The top panels, (a) and (b), show the vertical ($x - z$) and horizontal ($x - y$) slices through the accretion flow. Color shows the logarithm of density: red shows high and blue shows low values (see color bar). The black circle shows a BH ($a = 0.99$) and black lines show field lines. The bottom 3 panels show, from top to bottom, mass accretion rate, \dot{M} (panel c), dimensionless flux through the BH, ϕ_{BH} (panel d), and outflow efficiencies of the whole outflow, η (red solid line), the jet, η_{jet} (green dashed line), and the wind, η_{wind} (blue dash-dotted line) (panel e). Since η_{jet} and η_{wind} are measured at $r = 100r_g$, they lag by $\Delta t \approx 100r_g/c$ relative to η , which is measured at $r = r_{\text{H}}$. Colored symbols show values at the snapshot time, $t \approx 12305r_g/c$. At $t = 0$, the accretion flow contains a large amount of large-scale magnetic flux. Accretion brings mass and flux to the hole, and ϕ_{BH} increases until it reaches a maximum value at around $t \approx 6000$ time units. At this time the BH is saturated with magnetic flux and produces as much power as possible. However, the accretion flow brings in even more flux, which impedes the accretion and leads to a magnetically arrested disk. Some of the flux escapes from the BH via magnetic interchange and flux eruptions, two of which are seen in panels (a) and (b), which frees up room for new flux. This process continues in a quasi-periodic fashion, and on average the BH produces outflows at $\eta \approx 140\%$ efficiency, i.e., outflows carry more energy than the entire rest-mass energy supplied by accretion.

much higher values of η than previously reported [19]. In fact, $\eta > 100\%$, therefore jets and winds carry more energy than the entire rest-mass supplied by the accretion, and this unambiguously shows that *net* energy is extracted from the accreting BH. This is the first demonstration of *net* energy extraction from a BH in a realistic astrophysical scenario. Thicker MADs ($h/r \approx 0.6$)

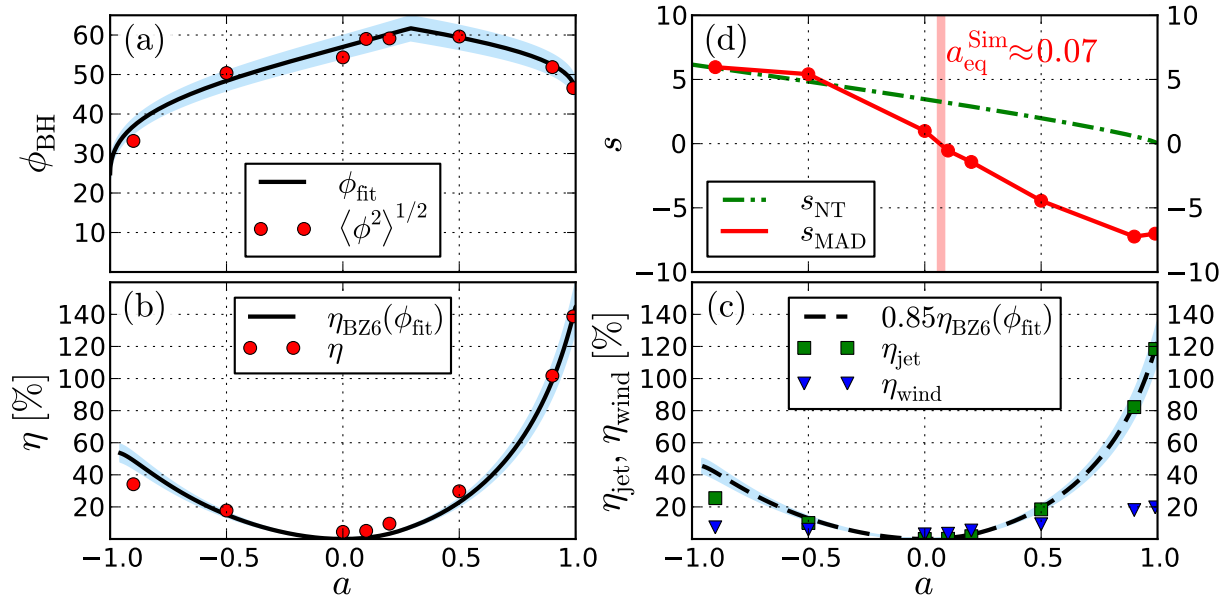


Figure 4. Spin-dependence of various quantities for MADs with $h/r \approx 0.3$. (a) Dimensionless BH spin, ϕ_{BH} : simulation results (red dots), by-eye fit, ϕ_{fit} , comprised of two linear segments in a $\phi_{\text{BH}}-\Omega_{\text{H}}$ plane (black line), and 5% uncertainty on the fit (blue band). (b) Energy outflow efficiency, η : simulation results (red dots), BZ6 efficiency (black line, eq. 2) assuming $\phi_{\text{BH}}(a) = \phi_{\text{fit}}(a)$, and 10% uncertainty (blue band). (c) Jet efficiency (green squares) and wind efficiency (inverted blue triangles). Dashed line shows 85% of the above BZ6 efficiency (a good estimate of jet power for prograde BHs [23]), and blue color shows a 10% uncertainty band. (d) BH spin-up parameter, s , for a thin Novikov-Thorne disk [38] (green dash-dotted line) and for the simulations (red dots). Whereas for thin disks the equilibrium value of BH spin is $a_{\text{eq}}^{\text{NT}} = 1$, for our simulations it is much lower, is $a_{\text{eq}}^{\text{Sim}} \approx 0.07$ (vertical red band).

produce outflows at an even higher efficiency, $\eta \simeq 300\%$ [24].

Importantly, in the MAD state η is independent of the initial amount of magnetic flux in the accretion flow, i.e., η depends only on BH spin, a , and disk density angular thickness, h/r [23]. This allows us to reliably study spin-dependence of various quantities, shown in Figure 4. Dimensionless BH flux, ϕ_{BH} , shows $\sim 50\%$ variation with spin (see panel a). Prograde BHs ($a > 0$) are a few times more efficient than retrograde BHs ($a < 0$) for the same value of $|a|$ (see panel b). Quite the opposite—10 times larger efficiency of retrograde BHs than of prograde BHs—is predicted by the “gap” model [39], which assumes that zero magnetic flux populates the “gap” between the BH horizon and the innermost stable circular orbit (ISCO). We find that this interpretation of the ISCO—as the surface inside of which all magnetic flux nearly freely falls into the BH—does not hold in MADs: interchange instability [40] and flux eruptions (see Fig. 3) populate the ISCO interior with flux. In fact, the thinner the disk, the larger the fraction of BH magnetic flux that resides in the region between the BH horizon and the ISCO [23, 24].

Panel (c) shows the division of total outflow efficiency into highly magnetized jet and weakly magnetized wind components, with efficiencies η_{jet} and η_{wind} , respectively. Since jets are BH spin-powered (eq. 2), for $a = 0$ jet efficiency vanishes, but winds still derive their power from an accretion disk via a Blandford-Payne-type mechanism [41]. The larger the spin, the more efficient jets and winds. For rapidly spinning BHs most of the energy—about 85% for prograde BHs—is carried by relativistic jets. Importantly, even rather slowly spinning BHs, with $a \lesssim 0.5$, produce prominent BH spin-powered jets. This is in agreement with the recent evidence that

jets in BHBs are powered by BH rotation over a wide range of BH spin, $0.1 \lesssim a \lesssim 0.9$ [42].

Do our highly efficient jets affect the spin of central BHs? Figure 4(d) shows spin-dependence of BH spin-up parameter, $s = M/\dot{M} \times da/dt$ [43]. For standard geometrically thin accretion disks, $s > 0$ (see Figure 4(d) and [38]), and the equilibrium spin is $a_{\text{eq}}^{\text{NT}} = 1$ [44] (we neglect photon capture by the BH, which would limit the spin to $a \approx 0.998$ [45]). Thick accretion flows in time-dependent numerical simulations [29, 43, 46] and semi-analytic studies [47] typically have $a_{\text{eq}} \sim 0.9$ (however, see [48]). Figure 4(d) shows that the equilibrium value of spin for our MADs (with $h/r \approx 0.3$) is much smaller, $a_{\text{eq}}^{\text{Sim}} \approx 0.07$, due to large BH spin-down torques by our powerful jets. Since jet efficiency is $\sim 10^3$ times lower at this value of spin than for rapidly spinning BHs, such equilibrium spin systems are possible candidates for RQ AGN.

4. Conclusions

We confirm that the standard BZ power formula, $P_{\text{jet}} \propto a^2$ (eq. 1), remains accurate only for $a \lesssim 0.5$ and present a higher order BZ6 approximation (eq. 2) that is accurate for all values of spin (see Figure 2). We find that if the BH magnetic flux is held constant, the presence of a thick accretion disk in low-luminosity AGN leads to a steep dependence of BH jet power on spin, $P_{\text{jet}} \propto \Omega_{\text{H}}^4$. This steep dependence allows to explain a factor of 10^3 radio loud/quiet dichotomy of AGN via having two galaxy populations different by the spin of central BHs.

We carried out a series of time-dependent global GRMHD simulations of BH accretion that contain a large amount of magnetic flux. We show that the accumulation of magnetic flux around the center can lead to the formation of a strong centrally-concentrated magnetic field that saturates the BH, obstructs the accretion, and leads to a magnetically-arrested disk (MAD, [19, 23, 24, 33–37]). We show that in this state the outflow efficiency, η , depends only on the BH spin, a , and the angular density thickness of the accretion flow, h/r , and is independent of the initial amount of magnetic flux in the disk. Since BH magnetic flux is as large as possible, we expect MAD systems to achieve the maximum η for a given BH spin and disk thickness. Indeed, we find highly efficient outflows, with $\eta \gtrsim 100\%$, which suggests that MADs might explain observations of AGN with apparent $\eta \sim \text{few} \times 100\%$ [6–11]. We determine the spin-dependence of jet, wind, and total efficiencies in our simulations (Figure 4) and expect that this information can be useful for calibration of semi-analytic jet power models, for studies seeking to infer BH spin from the observed jet efficiency, and for tests of general relativity [11, 49–52].

AT was supported by the Princeton Center for Theoretical Science fellowship. AT and RN were supported in part by NSF grant AST-1041590 and NASA grant NNX11AE16G. We acknowledge NSF support via TeraGrid resources: NICS Kraken and Nautilus, where simulations were carried out and data were analyzed, and NCSA MSS and TACC Ranch, where data were backed up, under grant numbers TG-AST100040 (AT), TG-AST080025N (JCM), TG-AST080026N (RN).

References

- [1] Blandford R D and Znajek R L 1977 *MNRAS* **179** 433–456
- [2] Chiueh T, Li Z Y and Begelman M C 1991 *ApJ* **377** 462–466
- [3] Heinz S and Sunyaev R A 2003 *MNRAS* **343** L59–L64
- [4] Tchekhovskoy A, McKinney J C and Narayan R 2008 *MNRAS* **388** 551–572
- [5] Tchekhovskoy A, McKinney J C and Narayan R 2009 *ApJ* **699** 1789–1808
- [6] Rawlings S and Saunders R 1991 *Nature* **349** 138–140
- [7] Ghisellini G *et al.* 2010 *MNRAS* **402** 497–518
- [8] Fernandes C A C *et al.* 2011 *MNRAS* **411** 1909–1916
- [9] McNamara B R, Rohanizadegan M and Nulsen P E J 2011 *ApJ* **727** 39
- [10] Punsly B 2011 *ApJ* **728** L17

- [11] Martínez-Sansigre A and Rawlings S 2011 *MNRAS* **414** 1937–1964
- [12] Sikora M, Stawarz L and Lasota J P 2007 *ApJ* **658** 815–828
- [13] Fender R P, Belloni T M and Gallo E 2004 *MNRAS* **355** 1105–1118
- [14] Wilson A S and Colbert E J M 1995 *ApJ* **438** 62–71
- [15] Moderski R and Sikora M 1996 *A&AS* **120** C591
- [16] Komissarov S S 2001 *MNRAS* **326** L41–L44
- [17] Tanabe K and Nagataki S 2008 *Phys. Rev. D* **78** 024004
- [18] Tchekhovskoy A, Narayan R and McKinney J C 2010 *ApJ* **711** 50–63
- [19] Tchekhovskoy A, Narayan R and McKinney J C 2011 *MNRAS* **418** L79–L83
- [20] Gammie C F, Narayan R and Blandford R 1999 *ApJ* **516** 177–186
- [21] Komissarov S S and Barkov M V 2009 *MNRAS* **397** 1153–1168
- [22] Penna R F *et al.* 2010 *MNRAS* **408** 752–782
- [23] Tchekhovskoy A and McKinney J C 2012 *arXiv:1201.4385*
- [24] McKinney J C, Tchekhovskoy A and Blandford R 2012 *arXiv:1201.4163*
- [25] McKinney J C 2005 *ApJ* **630** L5–L8
- [26] De Villiers J P, Hawley J F, Krolik J H and Hirose S 2005 *ApJ* **620** 878–888
- [27] Hawley J F and Krolik J H 2006 *ApJ* **641** 103–116
- [28] Barkov M V and Baushev A N 2011 *New Ast.* **16** 46–56
- [29] McKinney J C and Gammie C F 2004 *ApJ* **611** 977–995
- [30] Beckwith K, Hawley J F and Krolik J H 2008 *ApJ* **678** 1180–1199
- [31] McKinney J C and Blandford R D 2009 *MNRAS* **394** L126–L130
- [32] Balbus S A and Hawley J F 1991 *ApJ* **376** 214–233
- [33] Bisnovatyi-Kogan G S and Ruzmaikin A A 1974 *Ap&SS* **28** 45–59
- [34] Bisnovatyi-Kogan G S and Ruzmaikin A A 1976 *Ap&SS* **42** 401–424
- [35] Igumenshchev I, Narayan R and Abramowicz M 2003 *ApJ* **592** 1042–1059
- [36] Narayan R, Igumenshchev I V and Abramowicz M A 2003 *PASJ* **55** L69–L72
- [37] Igumenshchev I V 2008 *ApJ* **677** 317–326
- [38] Novikov I D and Thorne K S 1973 *In Black Holes-Les Astres Occlus, ed. C. De Witt & B. S. De Witt* (New York: Gordon & Breach)
- [39] Garofalo D 2009 *ApJ* **699** 400–408
- [40] Stehle R and Spruit H C 2001 *MNRAS* **323** 587–600
- [41] Blandford R D and Payne D G 1982 *MNRAS* **199** 883–903
- [42] Narayan R and McClintock J E 2012 *MNRAS* **419** L69–L73
- [43] Gammie C F, Shapiro S L and McKinney J C 2004 *ApJ* **602** 312–319
- [44] Bardeen J M 1970 *Nature* **226** 64–65
- [45] Thorne K S 1974 *ApJ* **191** 507–520
- [46] Krolik J H, Hawley J F and Hirose S 2005 *ApJ* **622** 1008–1023
- [47] Benson A J and Babul A 2009 *MNRAS* **397** 1302–1313
- [48] Moderski R, Sikora M and Lasota J 1998 *MNRAS* **301** 142–148
- [49] Daly R A 2011 *MNRAS* **414** 1253–1262
- [50] Buliga S D *et al.* 2011 *Astrophysics* **54** 548–552
- [51] Lei W H and Zhang B 2011 *ApJ* **740** L27
- [52] Bambi C 2012 *arXiv:1201.1638*